

4D imaging via remote refocus

 View On GitHub

 Download PDF

This project is maintained by [AMSIkking](#), and was funded by
[Calico Life Sciences LLC](#)

Appendix

Note that this is a limited PDF or print version; animated and interactive figures are disabled. For the full version of this article, please visit one of the following links:
https://amsikking.github.io/remote_refocus
https://andrewgyork.github.io/remote_refocus
https://calico.github.io/remote_refocus

Remote refocus enables class-leading spatiotemporal resolution in 4D optical microscopy

[Back to the main text](#)

Concept, rules and simulation

The idea

The basic concept of remote refocus is to make a 3D unity-magnification copy of the sample volume at a remote location, and then image this with a second microscope. Under normal operation, collecting light with a microscope objective away from the corrected focal plane will introduce aberrations that depend strongly on the effective defocus and give unacceptably poor 3D image quality [Pawley 2006]. The 'magic' of RR is to use a standard microscope setup (objective/tube lens) in combination with a reversed

copy of the optics (tube lens/objective) to produce an aberration-free 3D image - where the second microscope is configured to cancel the aberrations of the first. The detailed optical theory of RR is elegantly described in the original paper [Botcherby 2007] and will not be re-visited here. However, for those wishing to build an RR system, there are a few simple concepts and rules that should be highlighted.

Firstly there are two main optical arrangements (Figure A1) which we'll refer to as single objective remote refocus (SORR) and double objective remote refocus (DORR) for ease of discussion. DORR is the most straightforward implementation, and in its most elementary form consists of 3 identical microscopes back to back, where moving either the 2nd or 3rd objective will perform the refocusing. The simplest version of the SORR variant uses a single objective in a double pass configuration with an additional beam splitter optic and mirror. The re-focus in SORR is then performed by moving either the objective or the mirror.

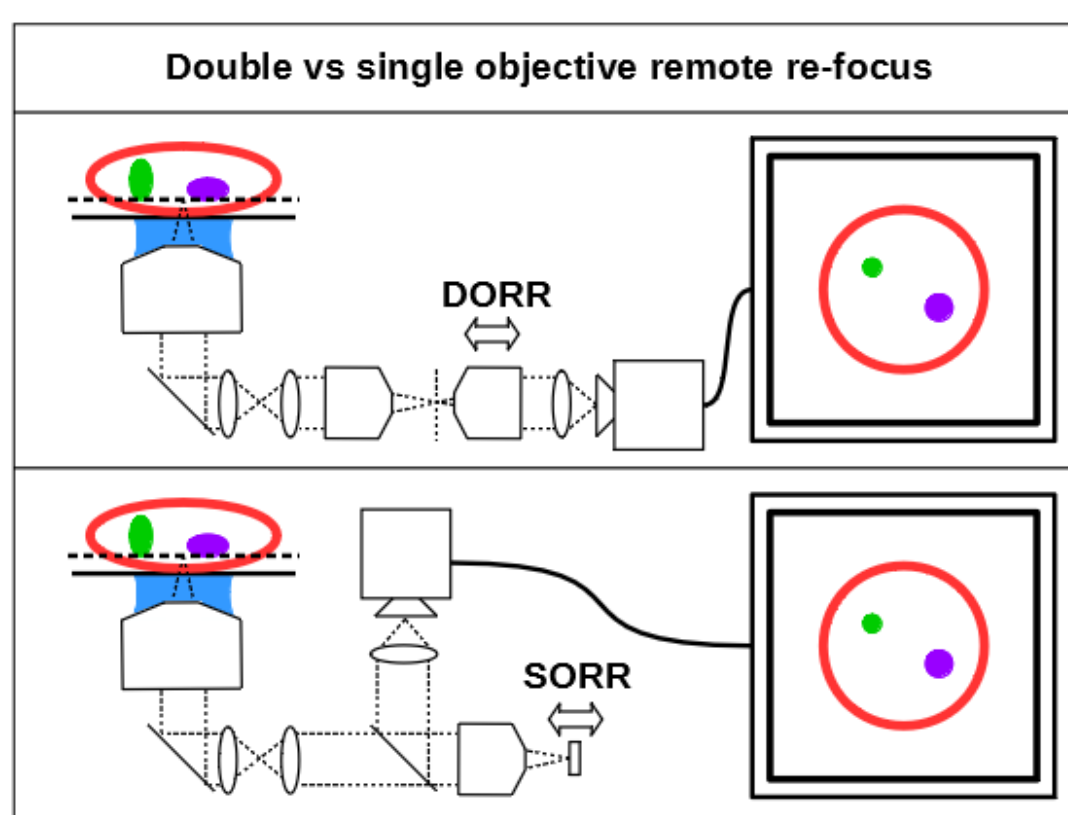


Figure A1: A schematic of the two basic remote refocus arrangements. Double objective remote refocus (DORR) vs. single objective remote refocus (SORR).

The main benefit of SORR is that the mirror can be very small and agile (<1 mm diameter) as it only has to cover the original sample scaled field of view (FOV), but the penalty is the introduction of the beam splitter optic. If a SORR is used with polarized

light then the introduction of a quarter wave plate and polarizing beam splitter cube can give high optical efficiency. However in most imaging modalities light is unpolarized and so the splitter optic in the SORR arrangement results in an immediate signal loss of 50% with a polarizing splitter and quarter wave plate, or 75% with a 50/50 splitter. Despite this loss the SORR arrangement has been implemented in many microscopes due to the potentially high speeds and the relative simplicity of the optical train as discussed in the [history](#) section. However if maximum efficiency is prioritized then the DORR arrangement is preferable and inherently faster in 'photon limited' applications, and for this reason the DORR arrangement was pursued in this work.

The golden rules

Secondly there are a number of '**golden rules**' for remote re-focus which must be respected to achieve best performance and are independent of the SORR or DORR arrangement.

1. The **magnification** between the sample and its remote 3D copy should be set **equal to the ratio of the index** between these two locations:

$$M_{RR} = \frac{n_{sample}}{n_{RR}}$$

For an air based RR system with $n_{RR} = 1$ then this gives $M_{RR} \approx 1.5$ for oil and $M_{RR} \approx 1.33$ for water, etc.

2. The optics downstream of the first objective should have **enough clear aperture** (CA) to accommodate the full wavefront as vignetting by any optic (tube lens or mirror etc.) will reduce resolution. It should be noted that the operation of RR expands the CA requirement beyond the normal range of a microscope, as defocused positions create non-infinity rays that may not be accommodated by the usual optical train. In this regard another critical consideration is that the RR objectives must have an angular acceptance that is greater than or equal to the first objective:

$$\frac{\text{NA}_{RR}}{n_{RR}} \geq \frac{\text{NA}_{sample}}{n_{sample}}$$

Again for an air based RR system with $n_{RR} = 1$ then this simplifies to:

$$\text{NA}_{RR} \geq \frac{\text{NA}_{sample}}{n_{sample}}$$

3. The **individual objectives and tube lenses** in the first two image relays which produce the 3D copy of the sample **should approximate ideal lenses**. RR theory is valid for lenses that well approximate ideal thin lenses placed in a 4f configuration, and deviating from this can have drastic effects on RR performance. It should be noted that not all objectives and tube lenses operate in this mode and so builders should choose their optics carefully. If you don't have detailed design information from your objective's manufacturer, we recommend you use the design we present here.

4. The tube lenses between the first and second objective in the system should be in a **telecentric 4f arrangement** to give **best performance**. On a typical commercial microscope stand this is often not the case, as the distance between the objective and tubes lens can be less than one focal length for practical reasons. This does not affect performance during normal use, but can degrade RR operation.

How to check

It should be noted that the aforementioned rules for remote refocus place substantial constraints on the optical design, and if followed carefully a well performing system can be built with relative ease, without the need for detailed optical design information or simulation. On the other hand, it can be difficult to know if a given objective is sufficiently "ideal". For those with access to detailed information about their optics and a suitable simulation software package like [Zemax](#) we recommend evaluating the performance of a possible RR configuration before building (Figure A2). Even for a novice designer this process can be relatively straightforward with the following workflow:

- Start by laying out a simple DORR optical train with ideal elements that match the diameters and focal lengths of the intended build and adhere to the '**golden rules**' of RR.
- Defocus the sample and chase the image with one of the RR objectives by the magnification factor between the conjugate planes (1st golden rule). The RR should work perfectly and any basic mistakes in design will be highlighted at this point and can be easily corrected.
- Now substitute in real components and evaluate the performance of the RR over its axial range. All of the non-idealities of the system will now show to give a finite range over which the real system can be expected to be diffraction limited (DL) if built and aligned correctly.

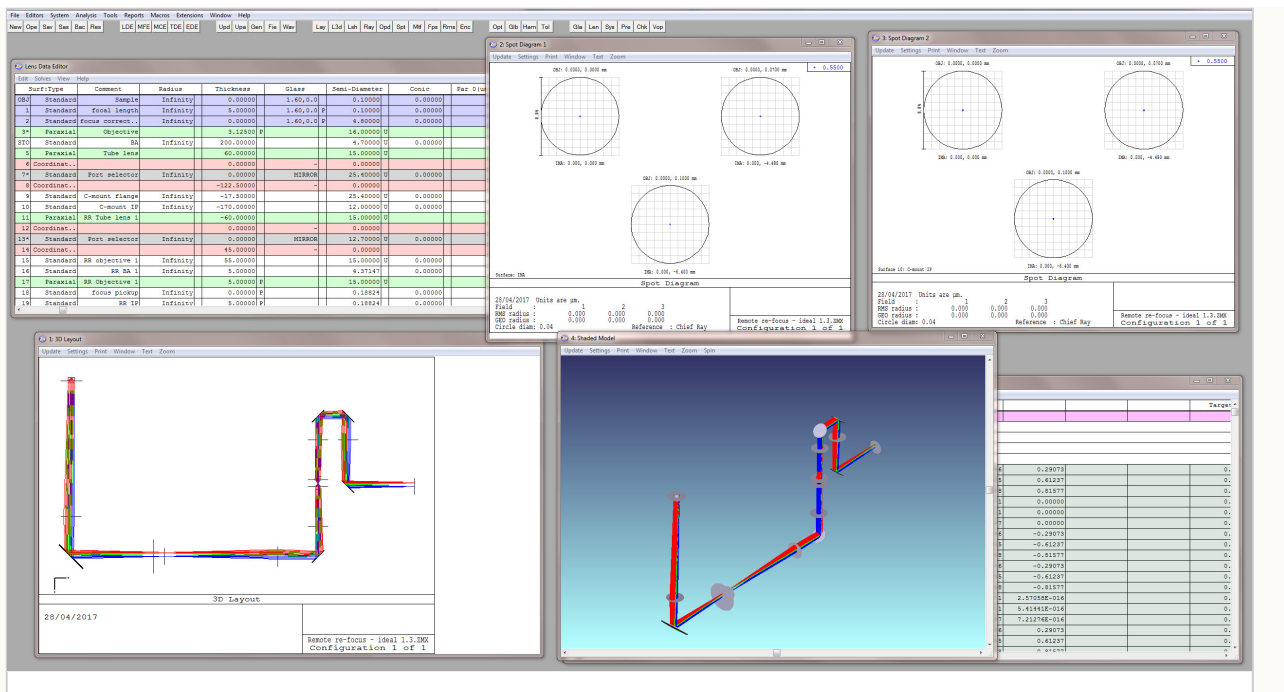


Figure A2: Zemax of remote refocus This figure shows the layout of the remote refocus using ideal lenses. The perfect lenses can then be substituted for real stock or manufactured lenses to evaluate optical performance.

Design

A high performance remote refocus for a 60x oil objective

In this section a recipe for a high performance remote refocus in the DORR configuration is given and presented as a versatile addition to a typical microscope stand. This RR module is designed to work with a high NA 60x oil immersion objective and is capable of producing multicolor DL stacks over the full FOV of a standard sCMOS camera. The emphasis in this design was on achieving a high performance RR using minimal custom parts. In this vein, all of the optics and the majority of the mechanics are relatively low cost, short lead time stock parts, with only a few simple bespoke mechanics where needed. The merits and choices of the design will now be discussed in turn and the reader may refer to the [build](#) section for a full [list of parts](#), [drawings](#) and an [alignment procedure](#).

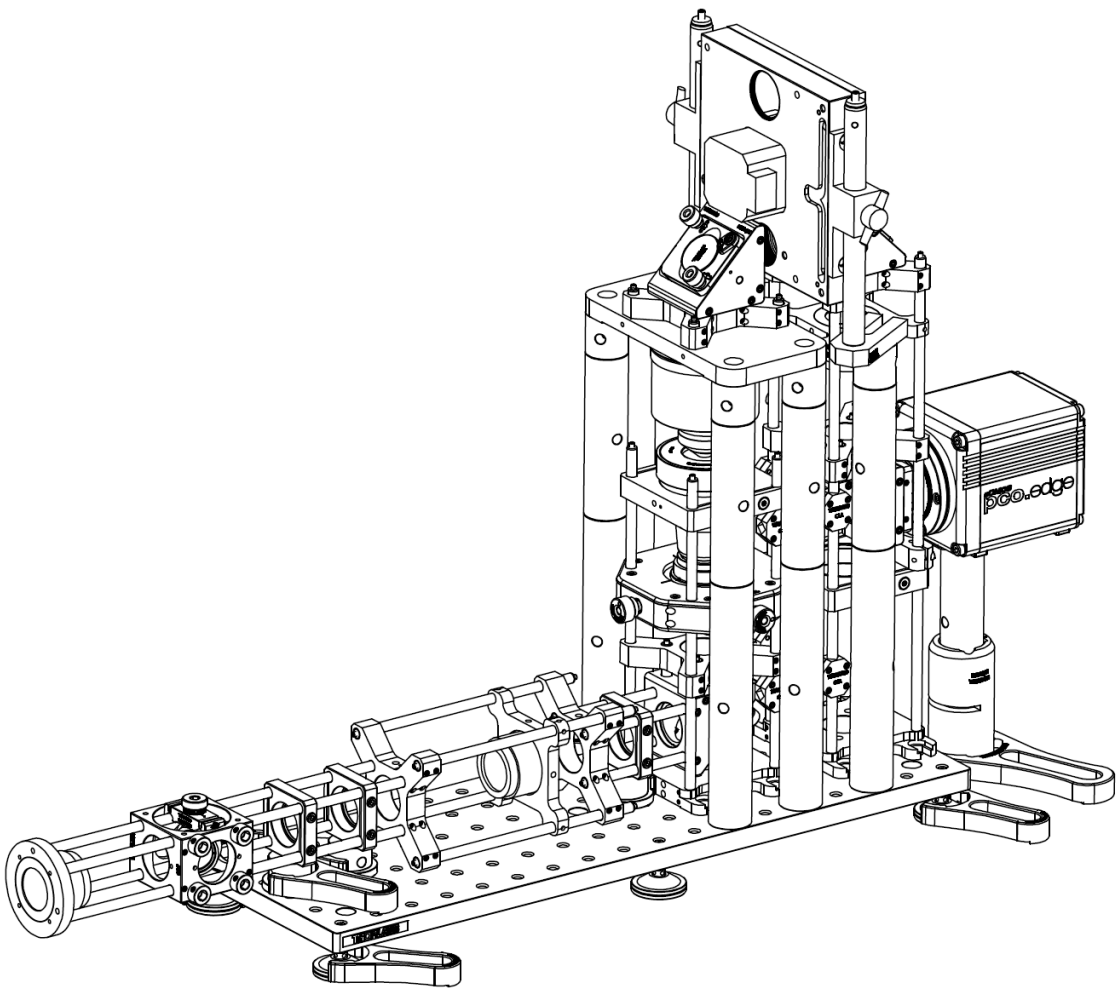


Figure A3: 3D CAD wireframe projection of the remote refocus. Modeling the mechanics of the remote refocus in CAD is straightforward, highly informative and recommended to potential builders.

To avoid custom optics, this DORR is based on the readily available [Nikon](#) 60x 1.4 NA oil and 40x 0.95 NA air objectives that, together with stock tube lenses, **very conveniently obey** the first three **golden rules** of RR, with the 4th rule achieved by setting the right mechanical spacing of the elements (see [drawings](#)). By working closely with [Nikon](#), we were able to establish excellent performance with a 450-650 nm polychromatic Strehl ratio >0.74 over an axial range of $\pm 32 \mu\text{m}$ in the sample with a $150 \mu\text{m}$ diameter field of view.

With good optical design established, the choice of Z-drive actuator was made relatively straightforward - an axial range of $\pm 32 \mu\text{m}$ in the sample with an index of ~ 1.5 corresponds to motion in air of $\sim \pm 50 \mu\text{m}$, which sits comfortably in the range of high performance piezo actuators - like the heavy duty [PI](#) 726 that can move a $\sim 200 \text{ g}$ objective at $>500 \text{ Hz}$ over a $100 \mu\text{m}$ range. The 726 can achieve step-and-settle times in the $0.1\text{-}1 \mu\text{m}$ range in $<10 \text{ ms}$ (Figure A3), which is faster than the rolling time of a good sCMOS camera like the [PCO.edge](#) 4.2 at full field of view. This equates to a running mode of 100 fps, giving 10 volumes per second for a 10-slice stack.

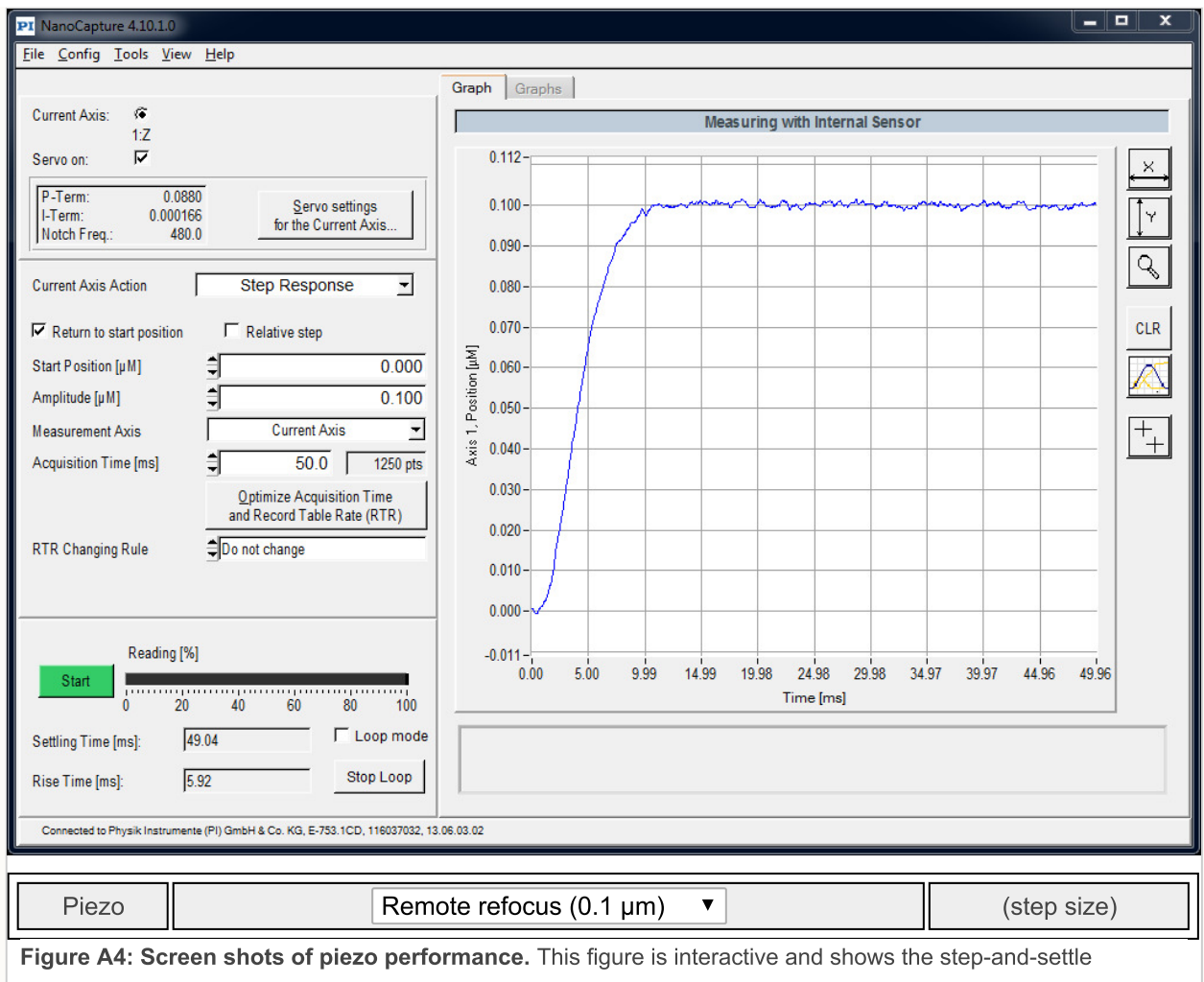


Figure A4: Screen shots of piezo performance. This figure is interactive and shows the step-and-settle performance of the piezo stage insert and remote refocus piezo for various parameters captured using the manufacturer's software and the built-in sensors on the devices. Note the 'Amplitude [μm]' box and the time (ms) on the x-axis for the blue line plot to settle.

Cropping the camera chip can produce higher frame rates for the fastest acquisitions, but in this regime the rolling time of the camera can be shorter than the step-and-settle time of the piezo, and motionless frames are no longer straightforward. It is straightforward, however, to operate the piezo in a constant-velocity mode, by sending a triangle wave signal to its analog input with an amplitude that corresponds to the desired stack size. The camera can then take frames at a high rate as the piezo moves continuously through the sample to give fast volumetric imaging but with an extended depth of field. It should also be noted that due to current limitations on sCMOS cameras the increased frame rates are achieved by cropping only one axis (up/down) with no benefit to cropping the second axis (left/right), and this forces elongated fields of view that may not be appropriate for all samples.

This motion solution prioritizes performance above economy, but may be substituted for other devices for those on a budget. Z-drive flexibility is a second-order advantage of using the RR arrangement - large, atypical actuators that would otherwise be awkward

to fit to a typical microscope can be accommodated with relative ease and do not interfere with normal operation of the stand.

The RR optics are folded with 4 standard 1" highly reflective mirrors, both to give a more compact footprint and also orientate the RR objectives into the vertical position for mechanical stability. The mirrors are housed in standard 3-axis kinematic mounts for ease of alignment and were noted to be slightly undersized at the design phase. This causes a small amount of vignetting in the corners of the sCMOS FOV at diameters >17.5 mm, but seemed like a good trade rather than upgrading to 2" mirrors and substantially increasing the size and cost of the module for relatively little gain. The fold arrangement accommodates common incubation chambers by keeping the optical train low and long out of the microscope side port, which is desirable for many live cell applications.

Another critical part of the design is the ability to align and stabilize the RR objectives, as unwanted motion here will translate directly into the image, making it the most sensitive part of the module. The Z-drive piezo/objective assembly is therefore mounted on a heavy-duty frame and isolated from the adjustable objective, which is mounted on an X/Y/Z translation stage to give the fine adjustment needed for alignment. Both RR objectives benefit from the gravitationally-aligned, axially symmetric vertical arrangement, which avoids many of the unwanted drifts and motions that can occur in alternative setups. Stability testing showed X/Y drifts in the 150 nm/hour range for the combined sample, stage, microscope and RR which seems acceptable given typical lab thermal drift and the intended sub-minute run time of a typical acquisition. All of the standard short lead-time optomechanics were sourced from [Thorlabs](#) and could be substituted for equivalent parts from existing lab stock.

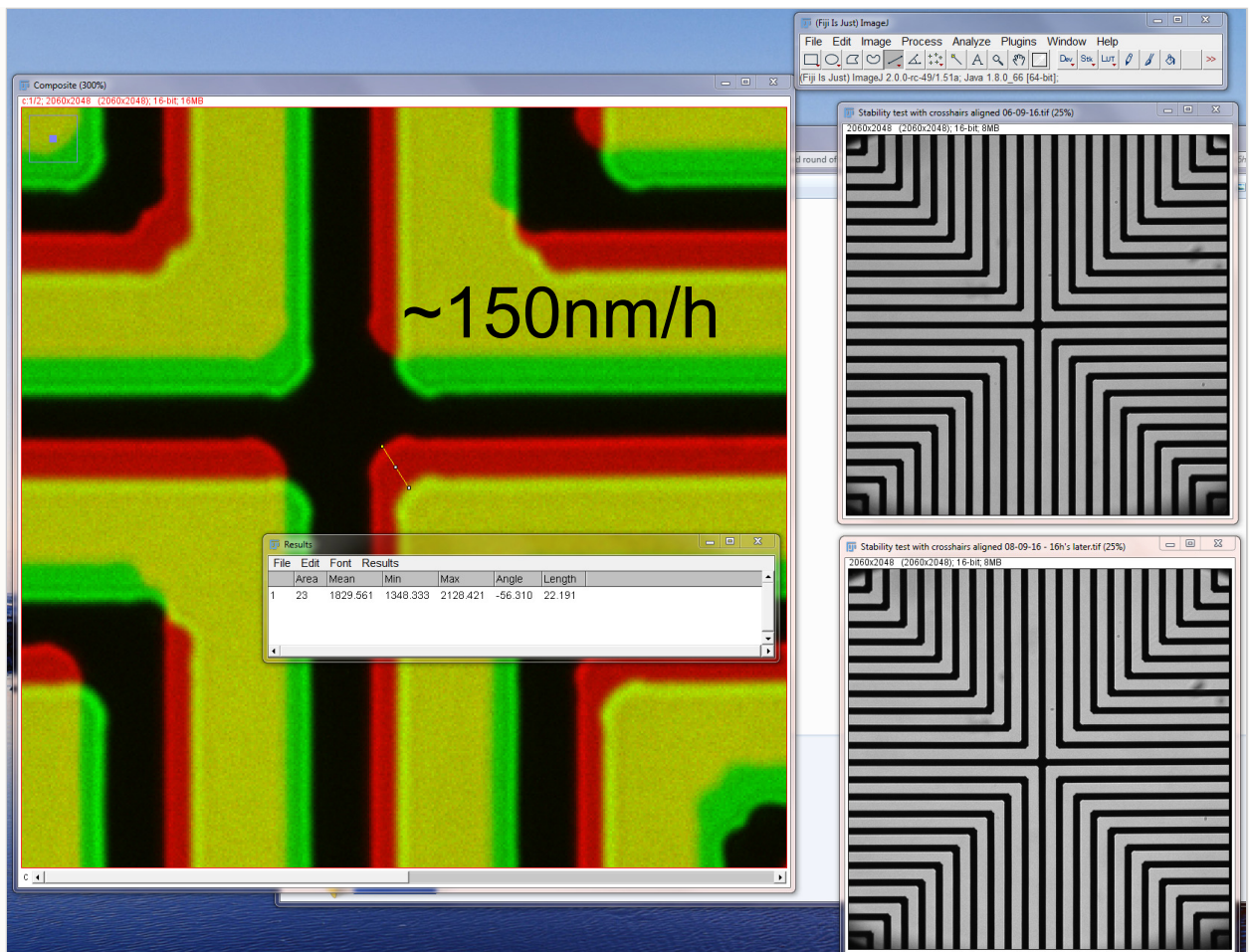


Figure A5: Stability testing showing 150 nm/hour drift. A graticule was imaged with the XY stage, RR piezo and microscope autofocus holding in closed loop control mode, with the difference between start and stop images shown by the red/green overlay.

An AR-coated 1" 340 µm coverslip correction glass window was ordered from [Mark Optics](#) and inserted between the two 40x air objectives to give best performance, as they are optimised to work with 170 µm of glass. An estimate for the optical efficiency of the RR was then calculated at ~70% with $(0.9^2)(0.95^2)(0.99^4)(0.99)$ for the objectives, tube lenses, mirrors and glass window respectively and was subsequently measured at >73% (Figure A6). For those looking to save on cost, the glass window can also be composed of two standard coverslips sandwiched together with some immersion oil, with the penalty of ~5% loss in signal.

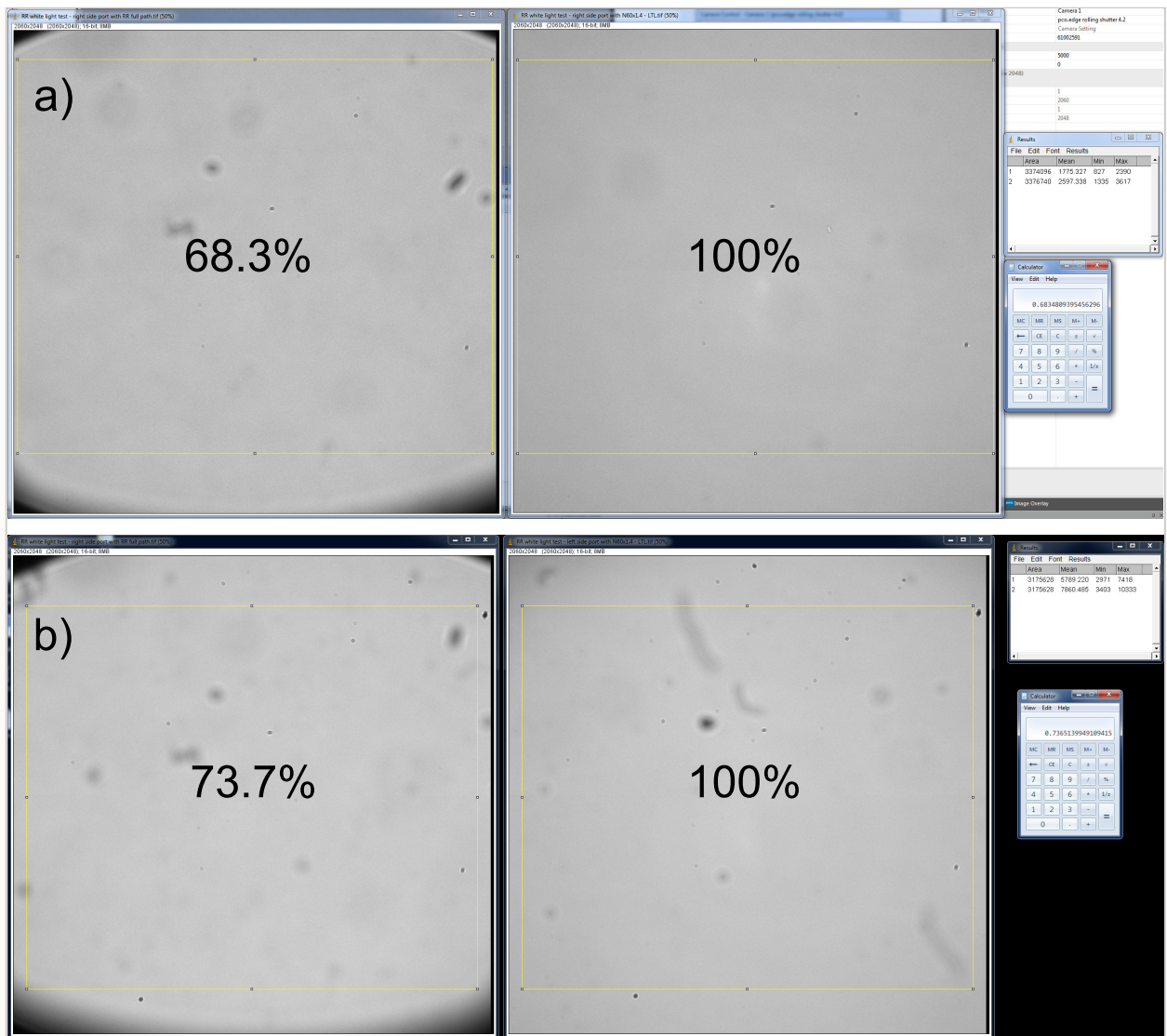


Figure A6: Optical efficiency tests show 73.7% transmission. The panels show broadband transmitted light images for the remote refocus port (left) and camera-only port (right) of the microscope. The RR efficiency is then given as the intensity ratio of these images for (a) two standard 170 μm coverslips sandwiched with oil between the RR objectives (68.3%), and (b) a custom 340 μm AR-coated glass window (73.7%).

A flexible slot was reserved in the infinity space behind the last objective for the inclusion of a high speed emission filter wheel like the [ASI FW-1000](#), which we chose for its high speed trigger options and <40 ms switching time. This can be mounted on the RR breadboard or directly to the optical table to avoid any unwanted vibrations that can couple from the torque generated by fast wheels. Of course, any filter wheel that physically fits can be used here - including a low-cost manual wheel from [Thorlabs](#) that will connect directly to the mechanics for starting off. The camera is easily focused by sliding the Z-position of the last mirror and orientated correctly with the built-in rotation mount, and the caged mirror on the input arm can be used to pull out the intermediate image plane without removing the instrument, if needed. The remaining custom parts were prepared by [Zera Development](#), but can be also readily milled by almost any CNC machine shop; see the [drawings](#) section for details. If you're unfamiliar with machine shops, simply send a copy of the drawing we provide to Zera.

Build

List of parts

This table can be used as a shopping list for the RR described in this article. Item 37 is a low cost manual filter wheel that can be substituted for an automated wheel if needed, and item 49 can be avoided to reduce cost (substitute with two coverslips sandwiched together with oil). With some re-design work, items 38-40 can be substituted for a lower cost option although this is not encouraged as it may negate the intended high speed operation of the device.

Item No.	Supplier	Part	Description	Qty
1	Thorlabs	MB1545/M	Aluminum Breadboard, 150 mm x 450 mm x 12.7 mm, M6 Taps	1
2	Thorlabs	SWB/M	Articulated Mounting Base, M6 x 1.0 Threaded Stud, Qty. 1	6
3	Thorlabs	ER10	Cage Assembly Rod, 10" (254.0 mm) Long, Ø6 mm	4
4	Thorlabs	C6W	30 mm Cage Cube, Ø6 mm Through Holes	1
5	Thorlabs	CP08/M	SM1 Threaded 30 mm Enhanced Clamping Cage Plate, 0.35" Thick, M4 Tap	3
6	Thorlabs	RS075P4M	Ø25.0 mm Pedestal Pillar Post, M4 Taps, L = 19 mm	3
7	Thorlabs	CF125	Short Clamping Fork, 1.24" Counterbored Slot, Universal	7
8	Thorlabs	LCP02/M	30 mm to 60 mm Cage Plate Adapter, M4 Tap	6
9	Thorlabs	ER6	Cage Assembly Rod, 6" (152.4 mm) Long, Ø6 mm	4
10	Thorlabs	ER3	Cage Assembly Rod, 3" (76.2 mm) Long, Ø6 mm	4
11	Thorlabs	ERSCA	Rod Adapter for Ø6 mm ER Rods, Qty. 1	4
12	Thorlabs	CP360R/M	Pivoting, Quick-Release, Ø1" Optic Mount for 30 mm Cage System (Metric)	1
13	Thorlabs	BB1-E02	Ø1" Broadband Dielectric Mirror, 400 - 750 nm	5
14	Thorlabs	CPVM	Vertical Cage System Mounting Plate	2
15	Thorlabs	ER8	Cage Assembly Rod, 8" (203.2 mm) Long, Ø6 mm	4
16	Thorlabs	KCB1C/M	Right-Angle Kinematic Mirror Mount with Smooth Cage Rod Bores, 30 mm Cage System and SM1 Compatible, M4 and M6 Mounting Holes	4

17	Thorlabs	ER1	Cage Assembly Rod, 1" (25.4 mm) Long, Ø6 mm	20
18	Thorlabs	CXYZ1/M	XYZ Translation Mount for Ø1" Optics, M6 Taps	1
19	Thorlabs	SM1A12	Adapter with External SM1 Threads and Internal M25 x 0.75 Threads	1
20	Thorlabs	LCP08/M	60 mm Cage Plate, SM2 Threaded, Enhanced Clamping, 0.5" Thick, M4 Tap (One SM2RR Retaining Ring Included)	2
21	Thorlabs	SM2V05	Ø2" Adjustable Lens Tube, 0.31" Travel	1
22	Thorlabs	SM2A6	Adapter with External SM2 Threads and Internal SM1 Threads	1
23	Thorlabs	RS150/M	Ø25 mm Post, L = 150 mm	6
24	Thorlabs	RS100/M	Ø25 mm Post, L = 100 mm	6
25	Thorlabs	RS25/M	Ø25 mm Post, L = 25 mm	6
26	Thorlabs	ER05	Cage Assembly Rod, 1/2" (12.7 mm) Long, Ø6 mm	12
27	Thorlabs	ER12	Cage Assembly Rod, 12" (304.8 mm) Long, Ø6 mm	4
28	Thorlabs	LCP01B	60 mm Cage Mounting Bracket	1
29	Thorlabs	SM1A39	Adapter with External C-Mount Threads and External SM1 Threads	1
30	Thorlabs	CRM1/M	Cage Rotation Mount for Ø1" Optics, SM1 Threaded, M4 Tap	1
31	Thorlabs	RS100/M	Ø25 mm Post, L = 100 mm	1
32	Thorlabs	RSH3/M	Ø25 mm Post Holder with Flexure Lock, Pedestal Base, L = 75 mm	1
33	Thorlabs	PF175	Clamping Fork for Ø1.5" Pedestal Post or Post Pedestal Base Adapter, Universal	1
34	Thorlabs	C1A	ER Rod Cross Coupler, Top and Bottom Pieces	8
35	Thorlabs	BA1S/M	Mounting Base, 25 mm x 58 mm x 10 mm	2
36	Thorlabs	TR150/M	Ø12.7 mm Optical Post, SS, M4 Setscrew, M6 Tap, L = 150 mm	2
37	Thorlabs	CFW6	30 mm Cage Filter Wheel for Six Ø1" Filters	1
38	PI	P-726.1CD	PIFOC® Ultra-High-Dynamics Microscope Lens Piezo-Z Positioning Drive, 100µm travel	1
49	PI	P-726.11	P-726 PIFOC® Thread Adapter M25	1
40	PI	E-753.1CD	High-Speed Single-Channel Digital Piezo Controller for	1

			Capacitive Sensors	
41	Nikon	MXA22018	Tube lens 200mm EFL	3
42	Nikon	MRD00405	CFI Plan Apo Lambda 40x - 0.95NA, WD0.25-0.16	2
43	Nikon	MRD01605	CFI60 Plan APOCHROMAT Lambda 60x Oil Immersion Objective Lens, N.A. 1.4, W.D., 0.13mm, F.O.V. 25mm, DIC	1
44	Zera Development	DMi8 casting flange adaptor 1.0	Adaptor for connecting a 6x30mm cage system to the cast flange of the DMi8 camera side port. This version is for the right hand port (left hand version requires M3 holes mirrored on optical axis).	1
45	Zera Development	Objective holder plate M25x0.75	Adaptor plate for integrating M25 x 0.75 objectives into a 6x60mm cage system with M6 counter sunk holes for metric breadboards. Exact thickness is design specific.	1
46	Zera Development	Tube lens adaptor M38 x 0.5 for 60mm cage 1.0	Adaptor plate for including M38 x 0.5 threaded parts into a 60mm cage system on axis.	2
47	Mark Optics	Custom	Custom glass window: Window, Coated, Bk-7, OD: 25mm +/- 0.2mm, Thk: 0.34mm +/- 0.1mm, polished both sides 20/10, TWF 1/4 wave, parallelism < 10 arc sec, CA 90%, VIS AR coated Tavg >99% 400-700nm, AOI = 0 degree	1

Drawings

For 2D CAD drawings please refer to this [folder](#), and for full-sized assembly drawings, please click [here](#). For our custom parts, .STEP files can be found [here](#) and 3D CAD for all other parts can be sourced from the respective manufacturers.

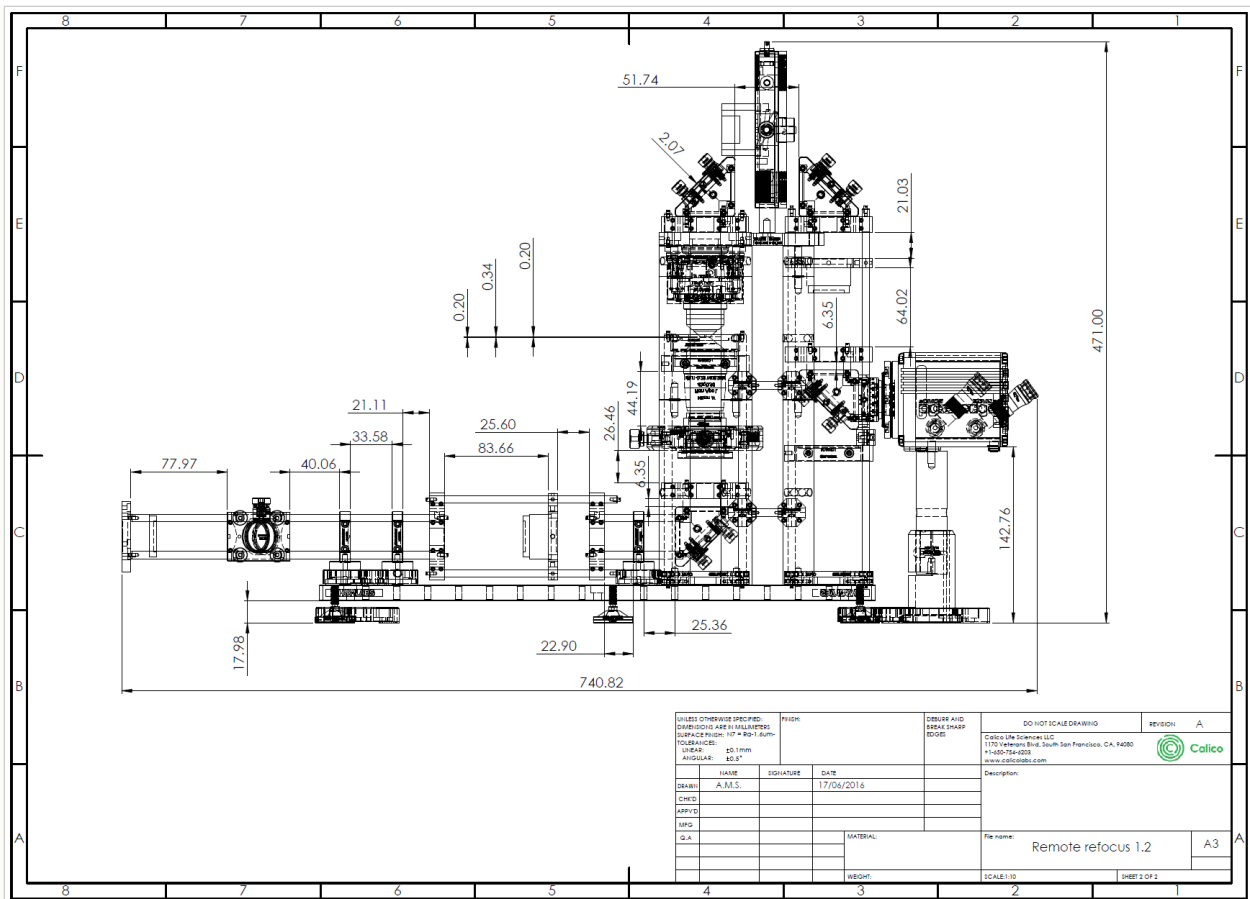


Figure A7: A wireframe assembly drawing for the remote refocus. The critical dimensions are shown in this drawing, which allows the builder to quickly align the system (full sized versions can be found [here](#)).

Alignment procedure

Aligning the RR for someone with optical assembly and microscopy experience is straightforward. For those unsure as to how to proceed, please try one of the following alignment procedures, bearing in mind that alignment is iterative and usually a learning process. The first time might take a day or two, the Nth time less than an hour...

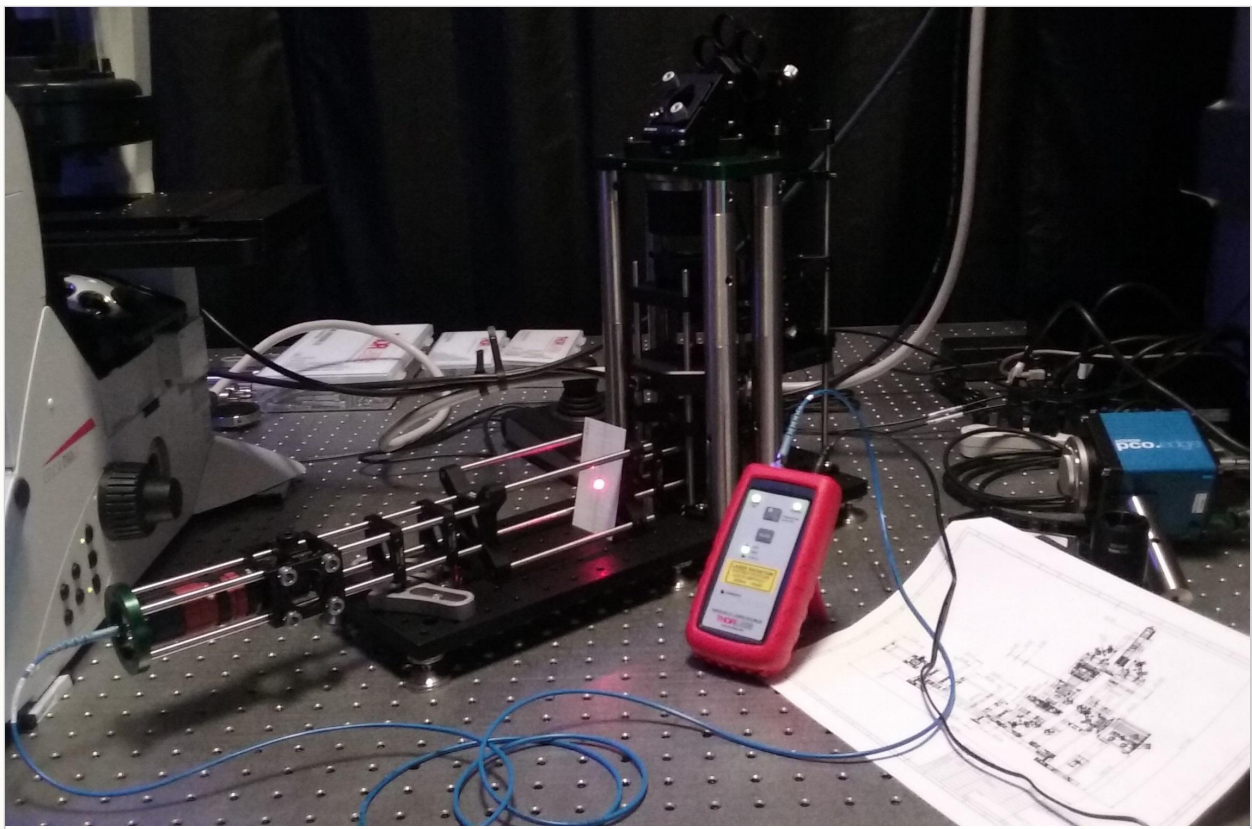


Figure 8: Alignment of the remote re-focus. This photo shows a fiber coupled laser being used to set the mirror alignment of the RR during the initial setup.

- Alignment with extended tool set and full access to components:
 1. Collimate a small diameter (<1 mm) low power (<1 mW) laser beam over a few meters and axially align the beam with the appropriate microscope thread (usually M25x0.75 or RMS).
 2. Remove all the lenses from the system (three objective/tube lens pairs) and the camera.
 3. Fire the laser beam through the microscope from the primary objective thread and out through the side port and through the RR optical train.
 4. Use pinholes or irises to firstly align the RR to the microscope by adjusting the height of the feet and the relative position on the table (then bolt down).
 5. Now use pinholes or irises to axially align the rest of the path using the RR tip tilt mirrors. At the end of this step the beam should be centered in X/Y at every point in the system from the primary objective to the camera.
 6. Now remove the laser, add the camera and fit the lenses as close as possible to their designed positions ready for imaging.
 7. Image a known sample (like a graticule) with transmitted light and focus with the eye pieces. Now image with the RR camera and (with the piezo powered and in its nominal rest position) use the X/Y/Z mount on the adjustable objective to focus and center the sample.

8. Now de-focus with the microscope stand and re-focus with the RR to check function. Minor adjustments to the mirrors and X/Y/Z objective may be needed for good alignment.

- Alignment with limited tools and access
 1. Image a known transmitted light sample (like a graticule) with the primary objective tube lens pair on the microscope using the eyepieces to centre and focus.
 2. Remove the RR lenses (two objective tube lens pairs) and the camera.
 3. Set the white light source to maximum intensity and darken the room so that the beam is visible throughout the system.
 4. Use pinholes or irises to firstly align the RR to the microscope by adjusting the height of the feet and the relative position on the table (then bolt down). A graticule with a well-chosen scale can have a visible image (crosshairs) that can be used at the magnified image plane to get good alignment.
 5. Now use pinholes or irises to axially align the rest of the path using the RR tip/tilt mirrors. At the end of this step the beam should be centered in X/Y at every point in the system, from the primary objective to the camera.
 6. Add the camera to the RR and fit the lenses as close as possible to their designed positions ready for imaging.
 7. Image with the RR camera and (with the piezo powered and in its nominal rest position) use the X/Y/Z mount on the adjustable objective to focus and center the sample.
 8. Now de-focus with the microscope stand and refocus with the RR to check function.
 9. Adjustments to the position of the RR base, mirrors and X/Y/Z objective will likely be needed for good alignment - expect to iterate.

Acquisition

Additional equipment

To evaluate the RR we used the following additional equipment in our experimental setup

Item No.	Supplier	Part	Description

1	Leica	DMi8	Research-grade inverted microscope stand with motorized Z-drive
2	PI	U-780	Automated XY stage, 100 nm precision, closed-loop PID control
3	PI	P-737	Z-piezo stage insert, 500 μm travel, 100 Hz resonant frequency (200 g load), closed loop PID control with 5 kHz analog-in
4	Lumencor	SpectraX	Multicolor LED light source with TTL trigger (10 μs rise/fall)
5	PCO	edge 4.2	sCMOS camera, 2048x2048 pixels with 6.5x6.5 μm^2 size, 100 fps full field, TTL trigger <50 μs response
6	NI	PCI-6733	8 channel analog-out card, 1 MHz, 16 bit
7	Zera Development	DMi8 stage spacer 15mm front 1.0	Raises XY stage on DMi8 platform by 15 mm to accomodate objectives with longer parfocal distance or piezo Z-drive inserts that require more height.
8	Zera Development	DMi8 stage spacer 15 mm rear 1.0	Raises XY stage on DMi8 platform by 15 mm to accomodate objectives with longer parfocal distance or piezo Z-drive inserts that require more height.
9	Thorlabs	PL15M25	15 mm Parfocal Length Extender for Microscope Objectives, M25 x 0.75 Threading

How we took our f

With the above mentioned hardware setup we used [Python](#) scripts to issue serial port commands to devices and create voltages to play with the [National Instruments](#) analog-out card. In practice, data was taken by focusing on the sample with the microscope Z-drive to give the ‘zero’ or reference position. Focus was then adjusted by using either the microscope Z, the piezo Z stage insert, or the remote refocus piezo depending on the mode of operation.

The original data presented in this article is available to download from [Zenodo \(17.5 GB, DOI: 10.5281/zenodo.1145453\)](#) and can be unzipped (27.3 GB) and used with the [figure generation](#) code to reproduce the figures in the main text.

Example code

Here we annotate a typical example of the script that was used for data collection. The exact script for each data set was not kept, as it amounted only to minor changes in stack amplitude, step size, exposure, etc., or changes in the order of operation or

routine depending on the experiment. Base examples of the scripts used for biological imaging and motion performance can be found in the [data generation folder](#), including the associated dependencies for running the hardware, with the exception of the microscope stand the control of which cannot be made public due to a proprietary API.

1. Necessary python modules are imported, followed by hardware control scripts. The program then checks if it's the 'main' program and if so imports the multiprocessing module needed for image_data_pipeline.py which runs the camera. A sensible level of verbosity is then set using the logger commands.

```
# Built-in Python modules
import time
import tkinter
# Third party, but highly standard Python module
import numpy as np
# Custom scripts we've written for hardware control
# See: https://github.com/AndrewGYork/tools
import ni
import leica_scope
import physik_instrumente
import image_data_pipeline
import lumencor
from pco import pco_edge_camera_child_process, legalize_roi

if __name__ == '__main__':
    import multiprocessing as mp
    import logging
    logger = mp.log_to_stderr()
    logger.setLevel(logging.INFO)
```

2. COM ports are assigned to the hardware with serial control, and analog-out channels are given to the camera, RR and light source:

```
### COM port assignment
dmi8_com_port = 'COM4'
rr_piezo_com_port = 'COM6'
epi_com_port = 'COM10'

### Analog out channel settings
ao_ch = {'camera' : 0,
          'rr_piezo' : 1,
          'spx_uv' : 2,
          'spx_blue' : 3,
          'spx_cyan' : 4,
          'spx_teal' : 5,
          'spx_green' : 6,
          'spx_red' : 7,}
ao_ch_name = {}
for name, index in ao_ch.items():
    ao_ch_name[index] = name
```

3. The user sets the choice of objective to be either the 40x 0.95 NA air or 60x 1.4 NA oil. The RR instrument was designed to work with both objectives, but the 'z_ratio' which is the amount the RR piezo needs to move in air to give a certain de-focus in the sample, changes according to the 1st golden rule of RR. In practice with the optics used, we found 0.98 to be correct for air and 1.42 for oil when imaging the Argolight slide. This was calibrated by de-focusing a known amount with the microscope and then seeing what piezo offset was needed to refocus.

```
### Objective choice
objective = 'oil' # Choose 'air' or 'oil'
# 'air':0.98 for best correction collar setting of 0.19 for Argolight
# 'oil':1.42
z_ratio = {'air':0.98, 'oil':1.42}[objective]
```

4. Acquisition parameters are chosen including stack amplitude, step size, number of colors, number of volumes to image, exposure time and file name format. Sensible bounds of memory buffer size and camera chip region-of-interest are asserted to avoid crashes.

```
### Stack parameters
stk_amp = 5 # set half amplitude of stack around current focus (um)
stk_step_size = 1 # set stack step size (um)
stk_num_steps = round(2 * stk_amp / stk_step_size) + 1
# RR stack conversion
rr_stk_amp = stk_amp * z_ratio

### Volumetric image information
num_vol = 2
num_colors = 2 # To change from 2 must edit voltage code
num_frames = stk_num_steps * num_vol * num_colors
assert num_frames < 1001 # Set sensible upper bound on buffer

### Illumination settings
t1_ao_ch = ao_ch['spx_green'] # take an epi channels for trans light
led_ao_ch = ao_ch['spx_cyan'] # set epi excitation color
led_intensities = {'uv':255, # set epi excitation intensities
                  'blue':255,
                  'cyan':255,
                  'teal':255,
                  'green':255,
                  'red':255,}

### Camera settings
exposure_ms = 20 # set exposure - includes rolling time (ms)
filename_format = '%s_%s_vol_%sum_stk_%sum_step_%sms_exp.tif'
                  # (led_ao_ch, num_vol, stk_amp, stk_step_size, exp_ms)
roi = legalize_roi({'top':1, # Be careful to choose a 'legal' roi!
##                      'left':1,
##                      'right':2060
})
```

5. The camera, analog-out card, microscope, LED light source and RR piezo are initialized. The camera is controlled through the `image_data_pipeline.py` module which simultaneously handles grabbing frames, displaying to screen and saving to disk using multiprocessing. The data rate for the analog-out card is set at least 10x higher than the fastest acquisition event to ensure synchronization, and the microscope tube lens turret is moved to an empty position so as to not obscure the remote refocus optics. The RR piezo is centered on its reference position and a 'position to voltage' function is defined for analog control:

```

### Initialize hardware
# Camera
idp = image_data_pipeline.Image_Data_Pipeline(
    num_buffers=1,
    buffer_shape=(num_frames,    # Buffer size for full volume series
                  roi['bottom']-roi['top']+1,
                  roi['right']-roi['left']+1),
    camera_child_process=pco_edge_camera_child_process)
idp.apply_camera_settings(
    exposure_time_microseconds=exposure_ms*1000,
    trigger='external_trigger',
    preframes=0,
    region_of_interest=roi)
ao = ni.Analog_Out(
    num_channels='all',
    rate=1e5,      # Voltages per second
    daq_type='6733',
    board_name='Dev1')
# Microscope
dmi8 = leica_scope.DMI_8_Microscope(dmi8_com_port)
dmi8.set_max_pos_magn(max_n=4)
dmi8.change_magn(4) # Set tube lens to empty position
# Epi light source
epi_source = lumencor.SpectraX(epi_com_port, verbose=False)
epi_source.set_intensity(**led_intensities)
# Remote re-focus piezo
rr_piezo = physik_instrumente.E753_Z_Piezo(which_port=rr_piezo_com_port,
                                              verbose=False)
rr_piezo.move(50) # Send piezo to default zero position (um)
rr_piezo._finish_moving()
rr_piezo.set_analog_control_state(True)
def piezo_volts_from_pos(desired_piezo_offset_um):
    piezo_position_abs = 50 + desired_piezo_offset_um
    piezo_analog_in_voltage = (piezo_position_abs - 50) / 5
    assert -10 <= piezo_analog_in_voltage <= 10
    return piezo_analog_in_voltage

```

6. A voltages vs. time array is created for each channel of the analog-out card for device control (the default is zero volts for channels that are not specified). The exposure time set in the acquisition section is split into camera rolling time (time needed for camera to initialize all pixels) and actual exposure time (time when the

LED can be on and data can be taken) with an additional 'jitter time' added to ensure the camera doesn't miss the next trigger after an exposure. With the timeline established, 'lights on' time windows and piezo movements can be given according to the acquisition parameters.

```
### Set up voltages for analog out control
# Camera timing information
TTL_HIGH_V = 3 # 3V TTL
rolling_time_s = idp.camera.get_setting('rolling_time_microseconds')*1e-6
exposure_time_s = idp.camera.get_setting('exposure_time_microseconds')*1e-6
jitter_time_s = 50e-6
assert rolling_time_s < exposure_time_s
jitter_pix = round(jitter_time_s * ao.rate)
assert jitter_pix > 1 # Helps ensure the camera won't swallow a trigger
start_pix = jitter_pix + round(rolling_time_s * ao.rate)
stop_pix = round(exposure_time_s * ao.rate)
# Create voltage list and voltage shape
voltages_list = [] # To fill with numpy arrays
voltage_shape = (stop_pix + jitter_pix, ao.num_channels)
# Create voltages for volumes
for v in range(num_vol):
    # Create voltages for stacks
    for rr_piezo_z in np.linspace(-rr_stk_amp, rr_stk_amp, stk_num_steps):
        # Create voltages for frames
        # Transmitted light
        tl_frame_voltages = np.zeros(voltage_shape, dtype=np.float64)
        tl_frame_voltages[:start_pix, ao_ch['camera']] = TTL_HIGH_V
        tl_frame_voltages[start_pix:stop_pix, tl_ao_ch] = TTL_HIGH_V
        tl_frame_voltages[:, ao_ch['rr_piezo']] = piezo_volts_from_pos(
            rr_piezo_z)
        voltages_list.append(tl_frame_voltages)
        # Epi led excitation
        led_frame_voltages = np.zeros(voltage_shape, dtype=np.float64)
        led_frame_voltages[:start_pix, ao_ch['camera']] = TTL_HIGH_V
        led_frame_voltages[start_pix:stop_pix, led_ao_ch] = TTL_HIGH_V
        led_frame_voltages[:, ao_ch['rr_piezo']] = piezo_volts_from_pos(
            rr_piezo_z)
        voltages_list.append(led_frame_voltages)
    rr_stk_amp = -rr_stk_amp # bidirectional z scanning for speed
# Combine voltages into single array
voltages = np.concatenate(voltages_list, axis=0)
```

7. This optional code is useful for capturing live biological events that are seen on-screen in a preview mode. The user can watch the sample in real time, and hit the acquire button when something interesting happens. The script turns on the light source and continuously runs the camera in a loop (displaying to screen), until the user closes the window at which point the acquisition begins immediately.

```
### Prepare and run livemode for preview of sample
# Turn on transmitted light
tl_on_voltage_shape = (10, ao.num_channels) # 10 time units wide
tl_ao_ch_high = np.zeros(tl_on_voltage_shape, dtype=np.float64)
tl_ao_ch_high[:, tl_ao_ch] = TTL_HIGH_V
```

```

ao.play_voltages(tl_ao_ch_high, force_final_zeros=False)
# Reset camera buffer for livemode
idp.apply_camera_settings(frames_per_buffer=1) # For livemode image
def live_mode():
    # Tell the camera to start trying to take an image
    idp.load_permission_slips(num_slips=1)
    idp.camera.commands.send([('force_trigger', {})])
    assert idp.camera.commands.recv() # Trigger must be successful
    # Wait for any previous image to finish:
    while len(idp.idle_data_buffers) == 0: idp.collect_permission_slips()
    tk.after(1, live_mode) # Re-schedule livemode
    # Set up event loop for livemode
    tk = tkinter.Tk()
    tkinter.Label(tk, text="Close window to take a volumetric series").pack()
##    tkinter.Button(tk, text="Snap", command=live_mode).pack()
    tk.after(1, live_mode) # Schedule 1st instance of live mode in event loop
    tk.mainloop() # Run event loop for livemode

```

8. The camera is reset after the preview mode, and the analog-out card now plays the pre-defined voltage arrays to run the acquisition and save files to disk.

```

### Reset camera properties for ao triggered stack
idp.apply_camera_settings(frames_per_buffer=num_frames) # Reset for volumes
# Wait for any previous file saving to finish:
while len(idp.idle_data_buffers) == 0: idp.collect_permission_slips()
# Tell the camera to start trying to take stacks and where to save
idp.load_permission_slips(
    num_slips=1,
    file_saving_info=[
        {'filename': filename_format %(ao_ch_name[led_ao_ch],
                                       num_vol,
                                       2*stk_amp,
                                       stk_step_size,
                                       exposure_ms)})])
while not idp.camera.input_queue.empty(): # Is the camera ready?
    pass # If not then hold ao play until camera is ready

### Play analog voltages
start = time.perf_counter()
ao.play_voltages(voltages)
end = time.perf_counter()
##    print('Time elapsed in seconds =', end - start)
##    input('hit enter to continue...')


```

9. Hardware elements are released, ready for the next acquisition:

```

### Close all objects
idp.close()
ao.close()
dmi8.close()
rr_piezo.close()

```

History

A summary of RR publications

Since the original RR paper [[Botcherby 2007](#)], there have been many publications that have used this technique for a variety of applications. The aim of this section is provide a very concise summary of these developments, to help the reader frame the use of RR within the field of microscopy.

[[Botcherby 2008](#)] applied a SORR to a spinning disk confocal microscope operating in an extended depth of field (EDF) mode to give Z-projections onto a single camera exposure. This had the advantage of achieving high frame rates due to a small scanning mirror, at the expense of ~50% of the fluorescence light, which is currently the main drawback of the SORR arrangement. A tilt mirror close to the back focal plane (BFP) was added to give angular variations of the EDF image over a small range giving an effective 3D perspective of the sample. [[Dunsby 2008](#)] modified the DORR concept to invent the oblique plane microscopy (OPM) modality, which enables light-sheet illumination and collection from a single high-NA objective. This breakthrough resulted in a true ‘single objective’ light sheet microscope, removing the many drawbacks of multi-objective systems but with the inherent limitation of lower effective resolution and collection efficiency due to the tilted arrangement of the optics. For oil immersion objectives, this equates to a maximum effective numerical aperture of about 1, with a ~50% loss in fluorescence signal.

[[Botcherby 2009](#)] used SORR in combination with a line-illumination and slit confocal microscope arrangement, including a secondary scanning mirror, to pack lines onto the camera and produce high frame rates in the meridional or Z-plane of the sample. This SORR setup had the usual drawback of ~50% signal loss due to the polarizing beam splitter (PBS) cube, but was a nice early demonstration of how RR can be appended to an existing imaging platform. [[Salter 2009](#)] demonstrated the use of SORR in a two-photon microscope for analysing liquid crystal dynamics in Z.

[[Hoover 2011](#)] used SORR with their differential multiphoton microscopy technique to give agile Z-adjustment, and [[Kumar 2011](#)] improved on the original OPM setup by coupling the excitation through the RR so that the light sheet and image plane can be simultaneously swept through the sample in a remote fashion to give inherently synchronized imaging at high volumetric frame rates. [[Anselmi 2011](#)] combined SORR with 3D holographic stimulation and introduced a novel tilt of the RR scan mirror that is similar in concept to the OPM setup, and allows imaging of tunable oblique planes in the sample. The paper also offers a thorough quantification of RR performance with the

optics used in the experiment confirming the analysis of the original paper [Botcherby 2007]. [Smith 2011] combine SORR with a traditional point-scanning two-photon microscope to give agile axial adjustment and the ability to create oblique excitation planes via high speed synchronized 3D point scanning.

[Botcherby 2012] optimise their SORR for a two-photon microscope for high acquisition rates and present relevant applications, and [Wu 2012] combine SORR with widefield fluorescence lifetime microscopy (FLIM) to give agile 3D performance.

[Qi 2014] perform a thorough simulation and experimental testing of SORR for long working distance objectives with findings that are in line with the original paper [Botcherby 2007].

[Bouchard 2015] use DORR in an OPM arrangement to untilt the image plane from their swept confocally-aligned planar excitation (SCAPE) microscope, and [Dean 2015] use SORR to give fast Z-scanning of a light sheet that is imaged by a second orthogonal objective in their axially swept light sheet microscope (ASLM). Because the SORR is on the excitation path with abundant coherent polarized light, there is no important loss from the PBS which nicely demonstrates the use of a penalty-free RR arrangement.

[Sikkel 2016] refine the inherently synchronized 2nd generation OPM arrangement by adding parallelised multicolour excitation and emission paths, quantifying the performance and demonstrating relevant applications. The overall collection efficiency from the combined efficiencies of the optical train and OPM arrangement was found to be ~20%. [Dean 2016] advance the ASLM concept to a diagonally-swept version by using SORR to scan a dithered gaussian lattice light sheet onto a coverslip that is arranged at a convenient angle for the dual objective system. [Rupprecht 2016] take a pragmatic approach to incorporating a platform-independent SORR into a laser scanning microscope to give agile axial scanning in a relatively economical format using a voice coil actuator that they refer to as a Z-scanning unit (ZSU).

References

1. [Pawley 2006] Handbook of Biological Confocal Microscopy, third edition; J. Pawley; Springer US, ISBN 978-0-387-25921-5, eBook ISBN 978-0-387-45524-2, (2006)
<https://doi.org/10.1007/978-0-387-45524-2>
2. [Botcherby 2007] An optical technique for remote focusing in microscopy; E.J. Botcherby, R. Juškaitis, M.J. Booth and T. Wilson; Optics Communications, vol

- 281(4), p880-887, (2007) <https://doi.org/10.1016/j.optcom.2007.10.007>
- 3. [Botcherby 2008] Real-time extended depth of field microscopy; E.J. Botcherby, M.J. Booth, R. Juškaitis and T. Wilson; Optics Express, vol 16(26), p21843-21848, (2008) <https://doi.org/10.1364/OE.16.021843>
 - 4. [Dunsby 2008] Optically sectioned imaging by oblique plane microscopy; C. Dunsby; Optics Express, vol 16(25), p20306-20316, (2008) <https://doi.org/10.1364/OE.16.020306>
 - 5. [Botcherby 2009] Real-time slit scanning microscopy in the meridional plane; E.J. Botcherby, M.J. Booth, R. Juškaitis and T. Wilson; Optics Letters, vol 34(10), p1504-1506, (2009) <https://doi.org/10.1364/OL.34.001504>
 - 6. [Salter 2009] Liquid Crystal Director Dynamics Imaged Using Two-Photon Fluorescence Microscopy with Remote Focusing; P.S. Salter, G. Carbone, E.J. Botcherby, T. Wilson, S.J. Elston and E.P. Raynes; Phys. Rev. Lett., vol 103(25), 257803, (2009) <https://doi.org/10.1103/PhysRevLett.103.257803>
 - 7. [Hoover 2011] Remote focusing for programmable multi-layer differential multiphoton microscopy; E.E. Hoover, M.D. Young, E.V. Chandler, A. Luo, J.J. Field, K.E. Sheetz, A.W. Sylvester and J.A. Squier; Biomedical Optics Express, vol 2(1), p113-122, (2011) <https://doi.org/10.1364/BOE.2.000113>
 - 8. [Kumar 2011] High-speed 2D and 3D fluorescence microscopy of cardiac myocytes; S. Kumar, D. Wilding, M.B. Sikkel, A.R. Lyon, K.T. MacLeod and C. Dunsby; Optics Express, vol 19(15), p13839-13847, (2011) <https://doi.org/10.1364/OE.19.013839>
 - 9. [Anselmi 2011] Three-dimensional imaging and photostimulation by remote-focusing and holographic light patterning; F. Anselmi, C. Ventalon, A. Bègue, D. Ogden and V. Emiliani; PNAS, vol 108(49), p19504-19509, (2011) <https://doi.org/10.1073/pnas.1109111108>
 - 10. [Smith 2011] Agitation-free multiphoton microscopy of oblique planes; C.W. Smith, E.J. Botcherby, M.J. Booth, R. Juškaitis and T. Wilson; Optics Letters, vol 36(5), p663-665, (2011) <https://doi.org/10.1364/OL.36.000663>
 - 11. [Botcherby 2012] Aberration-free three-dimensional multiphoton imaging of neuronal activity at kHz rates; E.J. Botcherby, C.W. Smith, M.M. Kohl, D. Débarre, M.J. Booth, R. Juškaitis, O. Paulsen and T. Wilson; PNAS, vol 109(8), p2919-2924, (2011) <https://doi.org/10.1073/pnas.1111662109>
 - 12. [Wu 2012] Optical refocusing three-dimensional wide-field fluorescence lifetime imaging microscopy; Q. Wu, S. Guo, Y. Ma, F. Gao, C. Yang, M. Yang, X. Yu, X. Zhang, R.A. Rupp and J. Xu; Optics Express, vol 20(2), p960-965, (2012) <https://doi.org/10.1364/OE.20.000960>

13. [Qi 2014] Remote-focusing microscopy with long working distance objective lenses; Y. Qi, M. Lei, Y. Yang, B. Yao, D. Dan, X. Yu, S. Yan and T. Ye; Applied Optics, vol 53(16), p3473-3478, (2014) <https://doi.org/10.1364/AO.53.003473>
14. [Bouchard 2015] Swept confocally-aligned planar excitation (SCAPE) microscopy for high-speed volumetric imaging of behaving organisms; M.B. Bouchard, V. Voleti, C.S. Mendes, C. Lacefield, W. B. Grueber, R.S. Mann, R.M. Bruno and E.M.C. Hillman; Nature Photonics, vol 9, p113-119, (2015)
<https://doi.org/10.1038/nphoton.2014.323>
15. [Dean 2015] Deconvolution-free Subcellular Imaging with Axially Swept Light Sheet Microscopy; K.M. Dean, P. Roudot, E.S. Welf, G. Danuser and R. Fiolka; Biophysical Journal, vol 108, p2807-2815, (2015) <http://dx.doi.org/10.1016/j.bpj.2015.05.013>
16. [Sikkel 2016] High speed sCMOS-based oblique plane microscopy applied to the study of calcium dynamics in cardiac myocytes; M.B. Sikkel, S. Kumar, V. Maioli, C. Rowlands, F. Gordon, S.E. Harding, A.R. Lyon, K.T. MacLeod and C. Dunsby; Journal of Biophotonics, vol 9(3), p311-323, (2016)
<http://dx.doi.org/10.1002/jbio.201500193>
17. [Dean 2016] Diagonally Scanned Light-Sheet Microscopy for Fast Volumetric Imaging of Adherent Cells; K.M. Dean, P. Roudot, C.R. Reis, E.S. Welf, M. Mettlen and R. Fiolka; Biophysical Journal, vol 110(6), p1456-1465, (2016)
<https://doi.org/10.1016/j.bpj.2016.01.029>
18. [Rupprecht 2016] Remote z-scanning with a macroscopic voice coil motor for fast 3D multiphoton laser scanning microscopy; P. Rupprecht, A. Prendergast, C. Wyart and R.W. Friedrich; Biomedical Optics Express, vol 7(5), p1656-1671, (2016)
<https://doi.org/10.1364/BOE.7.001656>



Hosted on
[GitHub Pages](#)